The James Webb Space Telescope: Mission Overview and Status

Matthew Greenhouse
Goddard Space Flight Center
Greenbelt, MD 20771
301 286-4517
matt.greenhouse@nasa.gov

***Abstract* —** The James Webb Space Telescope (JWST) is the scientific successor to the Hubble Space Telescope. It is a cryogenic infrared space observatory with a 25 m^2 aperture (6 m class) telescope that will achieve diffraction limited angular resolution at a wavelength of 2 um. The science instrument payload includes four passively cooled near-infrared instruments providing broad- and narrow-band imagery, coronography, as well as multi-object and integral-field spectroscopy over the $0.6 < \lambda < 5.0$ μm spectrum. An actively cooled mid-infrared instrument provides broad-band imagery, coronography, and integral-field spectroscopy over the $5.0 < \lambda < 29$ μm spectrum. The JWST is being developed by NASA, in partnership with the European and Canadian Space Agencies, as a general user facility with science observations proposed by the international astronomical community in a manner similar to the Hubble Space Telescope. Technology development and mission design are complete. Construction, integration and verification testing is underway in all areas of the program. The JWST is on schedule for launch during 2021.

TABLE OF CONTENTS

1. DESIGNING FOR DISCOVERY

The science motivation for the JWST mission was developed by a succession of international science working groups and is described by Gardner, et al. 2006 & 2012, and Kalirai 2018 with updates maintained by the JWST flight science working group at: https://jwst.nasa.gov/science.html . This science case forms the basis from which detailed science and mission requirements were derived to guide engineering design and development of the JWST. The science observations that are implemented by the JWST will be proposed by the international astronomical community in response to annual peer reviewed proposal opportunities (Rigby 2012). The discovery potential of the JWST relative to other concurrent facilities is discussed in Thronson, Stiavelli, and Tielens 2009.

The emergence of the first sources of light in the universe marks the end of the "Dark Ages" in cosmic history (Rees 1997). The ultraviolet radiation field produced by these sources created the ionization that is observed in the local intergalactic medium (IGM). The JWST design provides unique capability to address key questions about this era in cosmic evolution including: what is the nature of the first galaxies; how and when did ionization of the space between them occur; and what sources caused the ionization? The JWST architecture is primarily shaped by requirements associated with answering the above questions.

In contrast to the Hubble Space Telescope (HST), the JWST is designed as an infrared optimized telescope to observe the redshifted visible and ultraviolet radiation from the first galaxies and supernovae of the first stars. To achieve the nJy sensitivity needed to observe this era ($z \sim 6$-20), the observatory must have a telescope aperture that is larger in diameter than the largest rocket faring, and the entire optical system must be cooled to ~40-50 K. Finally, the resulting large deployable cryogenic telescope must achieve HST-like angular resolution, but at a 4X longer wavelength thus, also necessitating a large diameter telescope aperture. The major observatory design features (Table 1, Figure 1) trace directly from these requirements and differ markedly from those of the HST.

The JWST science instrument payload is designed to probe the first galaxies with high angular resolution near-infrared image surveys in broad-band filters. This capability enables identification of primeval galaxies by searching for their Lyman continuum break with multi-filter photometry. This prominent feature occurs in the near-infrared (1.3 – 2.6 μm) for galaxies with redshifts in the range of 10 – 20. This broad-band technique exploits the maximum sensitivity of the observatory, such that the space density of galaxies can be probed to z~20. JWST high angular resolution imagery across the 0.6 – 29 μm spectrum will probe the assembly and evolution of galaxy morphologies to permit observation of when and how the Hubble morphological sequence formed.

The JWST is designed to enable near-infrared multi-object spectroscopy of thousands of galaxies at several spectral

Table 1: Key design parameters of the JWST and HST		
Performance Parameter	**HST**	**JWST**
OTE Diameter (meters)	2.4	6.1 by 6.6
Mass (kg)	11600	6330
Output power at load input (watts)	2400	2079
Unobscured Aperture (sq meters)	4.5	25
Overall optical transmission (%)	45 to 25	62 to 43
Telescope field of view (arc min)	14.6 (radius)	18 by 9
Wavelength of diffraction limited performance	0.5	2
Rayleigh radius (arc sec)	0.043	0.069
Telescope Strehl ratio (%)	80	80
Pointing accuracy without fine guidance (arc sec)	22	7
Pointing stability with fine guidance (arc sec)	0.007	0.007
Detector pixels (Mega pixels)	25	66
Data volume (Gbits/day)	27	458

resolutions (~10^2, ~10^3). This capability will enable users to probe the chemical evolution and metallicity of galaxies and the ionization state of the IGM across cosmic time. Low resolution multi-object spectroscopy will facilitate calibration of photometric redshifts for primeval galaxy studies. The JWST spectrometers include integral field capability over the 0.6 – 29 μm spectrum that will enable detailed spectral, morphological, and kinematic studies of high redshift galaxies and local galaxy nuclei. JWST spectroscopy includes wide field slitless grism spectroscopy to enable high redshift emission line galaxy surveys and spectroscopy of extrasolar planet atmospheres.

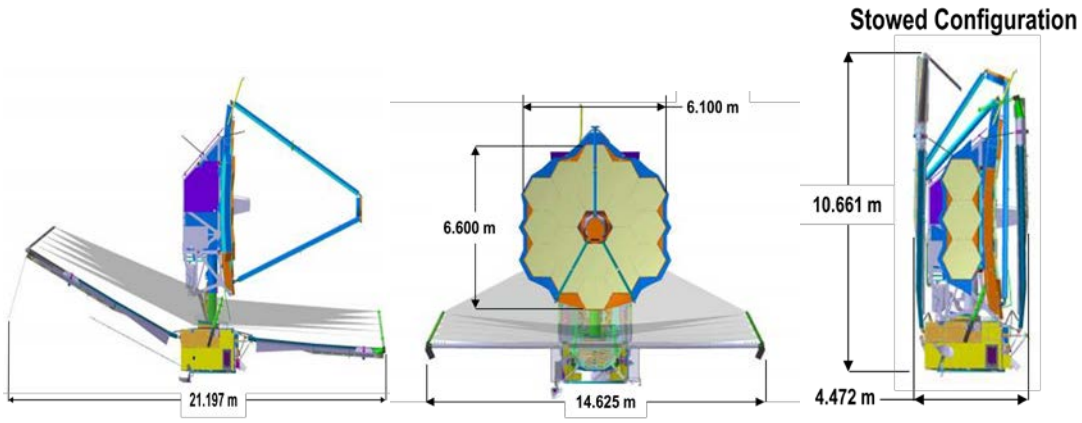

Figure 1: The JWST is the largest cryogenic optical system ever constructed

The JWST observatory design enables wide discovery potential beyond cosmology and galaxy studies. The JWST high angular resolution imagery and imaging spectroscopy across the 0.6 – 29 μm spectrum will open a new window on observation of star formation in our own galaxy to reveal: how molecular clouds collapse; how environment affects star formation and vice-versa; the mass distribution of low mass stars; and the relationship between stellar debris disks and the formation of terrestrial planets.

The JWST instruments include chronographic imagery, sparse aperture interferometry, and spectroscopy capability that will facilitate a wide range of stellar debris disk studies and extra-solar planet observations at high angular resolution. High dynamic range modes of the JWST instruments will enable extra-solar planet transit photometry and spectroscopy across the above wavelength range. The JWST observatory provides non-sidereal tracking so that the full observatory capability can be used to observe the outer solar system to enable comparative studies among stellar debris disks, extrasolar planets, and our own solar system.

2. ARCHITECTING FOR SUCCESS

The large primary mirror area and cryogenic operating temperature are key drivers on the JWST mission architecture. The telescope is the largest space telescope ever constructed. Liquid cryogen cooling techniques used by prior infrared space observatories (IRAS, ISO, and Spitzer) cannot be practically scaled to meet JWST requirements, and existing cryo-cooler technology could not meet the heat lift requirements of this large system. As a consequence, a passively cooled architecture was adopted for the majority of the system.

A libration point orbit about the Sun-Earth L2 point was selected to facilitate this approach to cooling the observatory (Figure 2). This choice enables the observatory and the earth to have the same period in their heliocentric orbit about the around the sun, such that the telecommunications range between the earth and the JWST remains constant throughout the mission. In addition, the primary sources of heat (sun and earth) always appear in the same direction. Hence, it is possible to continuously shield portions of the observatory from the sun and earth to provide passive cryogenic cooling.

The orbit about the L2 point itself is sized to ensure that the JWST never enters the Earth's shadow; thus enabling continuous generation of power with solar arrays. This orbit has a period of approximately 6 months and is unstable in the direction of the Earth-Sun line, requiring use of station-keeping thrusters. Propellant for orbit maintenance and momentum management ultimately limits the lifetime of the observatory to approximately twice the duration of its required 5 year science mission.

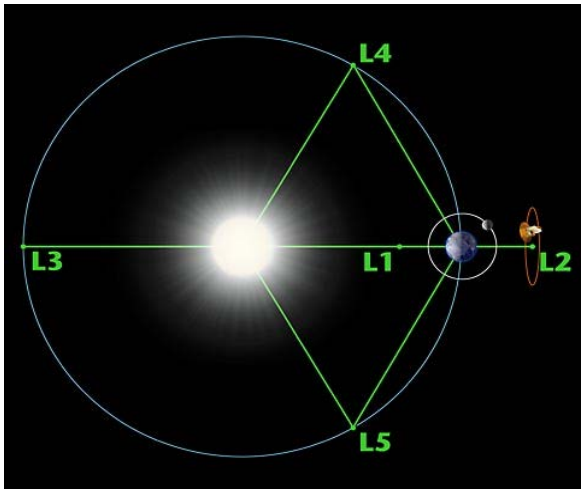

Figure 2: The location of the JWST libration point orbit relative to the Earth, Moon, and Sun.

The JWST can observe the whole sky while remaining continuously in the shadow of its sun shield. The space vehicle can pitch through an angle of 50 degrees and rotate completely about the earth-sun line to observe sources within an annulus that covers approximately 35% of the sky (Figure 3). As the observatory orbits the sun, this annulus sweeps over the whole sky every 6 months yielding small continuous viewing zones at the ecliptic poles.

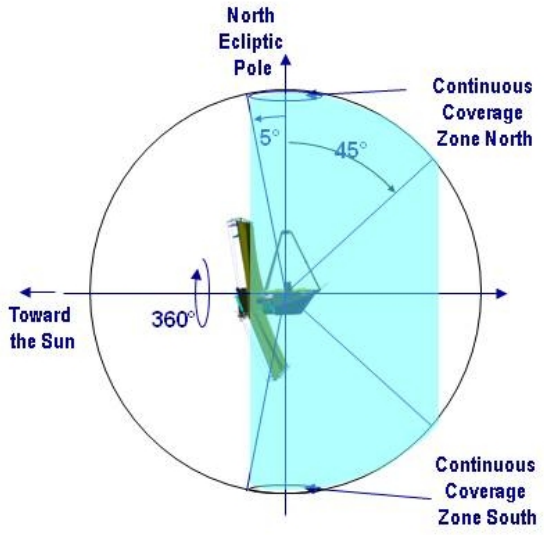

Figure 3: The JWST can observe 35% of the sky at any instant while remaining in the shadow of its sunshield. This annular field of regard covers the whole sky as the Earth orbits the Sun

The JWST will reach this orbit in approximately 100 days after launch from Guiana Space Center in French Guiana using an Ariane 5 ECA launch vehicle via a direct transfer trajectory. The 6.5 m diameter telescope and its tennis-court-sized sunshield, are designed to be stowed within the 5 m diameter Ariane rocket fairing along with the science instrument payload and spacecraft such that the observatory can deploy into its operational configuration (see animation at: https://youtu.be/bTxLAGchWnA). This process involves 40 deployable structures and 178 release mechanisms. The observatory is launched warm, and cooling begins after sunshield deployment in route to the L2 point.

During operations, the NASA Deep Space Network is used to support two 4 hr communications contacts each day during which approximately 458 Gbits of science data are downloaded. Both mission and science operations are supported by the Space Telescope Science Institute, which is currently operating the Hubble Space Telescope. Overall mission management, as well as guidance, navigation, and control, are provided by the NASA Goddard Space Flight Center.

3. COLLECTING THE FIRST LIGHT

A three mirror anastigmat (TMA) telescope design (Figure 4) was selected to provide high image quality over a wide field of view (Lightsey 2012). In contrast to ground-based telescopes, minimizing mass is a key design driver on the

JWST telescope. Beryllium was selected as a material for the three TMA mirrors due to its low expansion coefficient at the ~50K operating temperature (to enable high figure stability), high thermal conductivity, and high stiffness to mass ratio. A segmented primary mirror design was chosen to enable fold-up stowage (Figure 1). The deployed aperture is tricontagon in shape with an unobscured collecting area of 25 m^2. The primary mirror is composed of 18 hexagonal segments (1.32 m flat-to-flat) of three optical prescriptions.

Each primary mirror segment and the secondary mirror are mechanized to provide in-flight position adjustment in 6 degrees of freedom. The primary mirror segments also have capability for in-flight radius of curvature adjustment. A fine steering mirror is located near a pupil position. This mirror is servo controlled using an image-based fine guidance sensor located in the science instrument focal plane to enable 7 milliarcseconds rms pointing stability. The mirrors are polished to a cryogenic figure error of approximately 20 nm rms via an iterative polishing and cryogenic test process (Gallagher 2011). Gold was selected as a mirror coating to provide high throughput over the 0.6 - 29 micron spectrum. This coating choice limits the JWST to wavelengths >0.6 um. The 29 μm long wavelength limit results from detector technology and cooling constraints. Manufacturing, coating, and final cryogenic testing of all telescope mirrors has been completed (Figure 5). Their performance has been verified

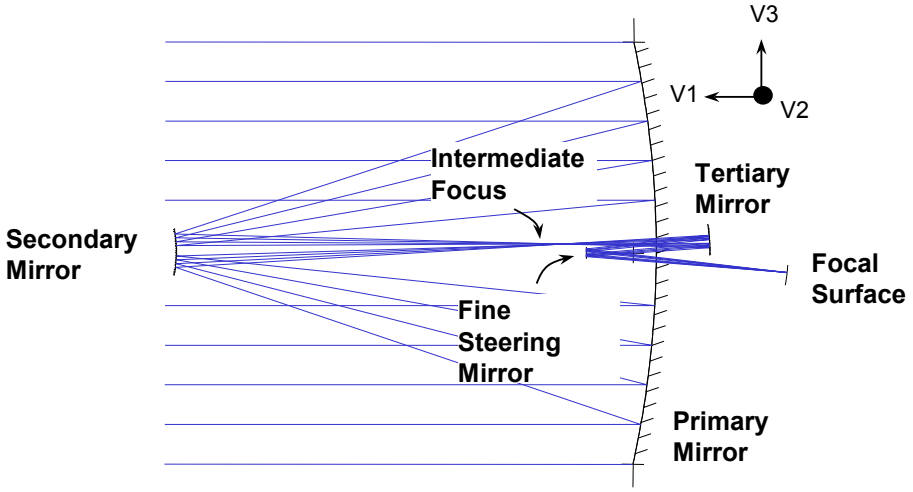

Figure 4: The telescope deploys into a three anastigmat configuration employing a fine steering mirror to enable 7 milliarcsecond line of sight pointing stability

Figure 5: All JWST telescope mirrors are completed and are within specification in every respect. From left to right: 1 of 18 primary mirror segments; the secondary mirror; the tertiary mirror; and the fine steering mirror.

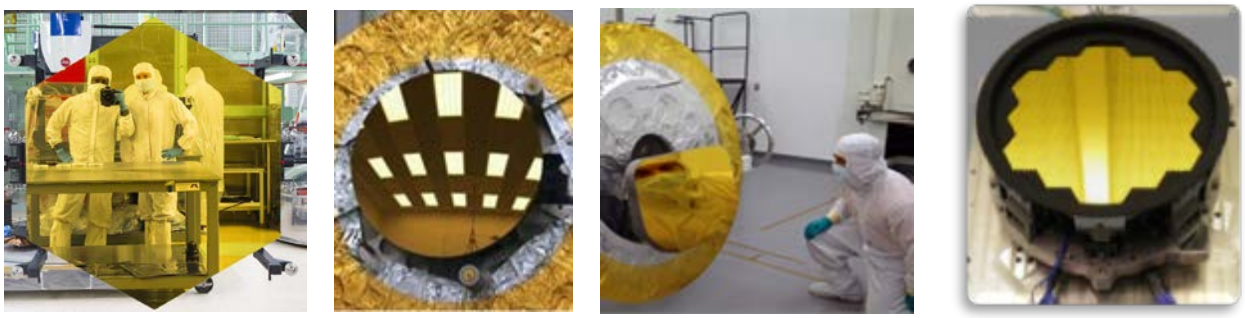

through test to be within specification in every respect (Feinberg et al. 2012).

The mirror segment actuators are periodically adjusted in flight to ensure diffraction limited image quality throughout the mission. The observatory's main near-infrared science camera (Section 4) is used as the wavefront error sensor for this process. Initial coarse phasing of the segments is accomplished using dispersed Hartman sensing optics in this camera (Figure 6). The subsequent fine phasing is performed on defocused images using a modified Gerchberg-Saxton algorithm (Acton 2004 & 2012). This process is designed to achieve a telescope Strehl ratio of 0.8 at a wavelength of 2 um.

Figure 6: Dispersed Hartman sensing optics within the NIRCam science instrument are used to perform coarse phasing of the primary mirror segments during flight.

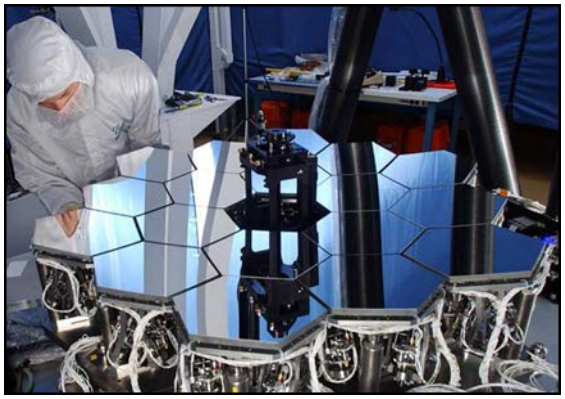

Figure 7: A 1/6th scale fully functional model of the JWST telescope was used to develop the overall telescope wavefront sensing and control algorithms

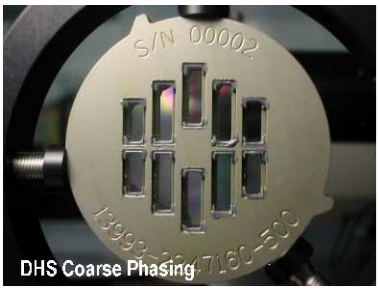

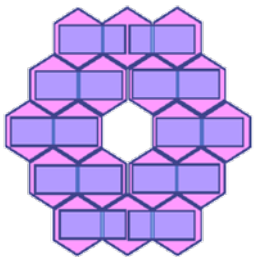

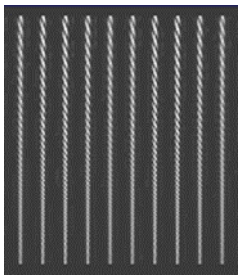

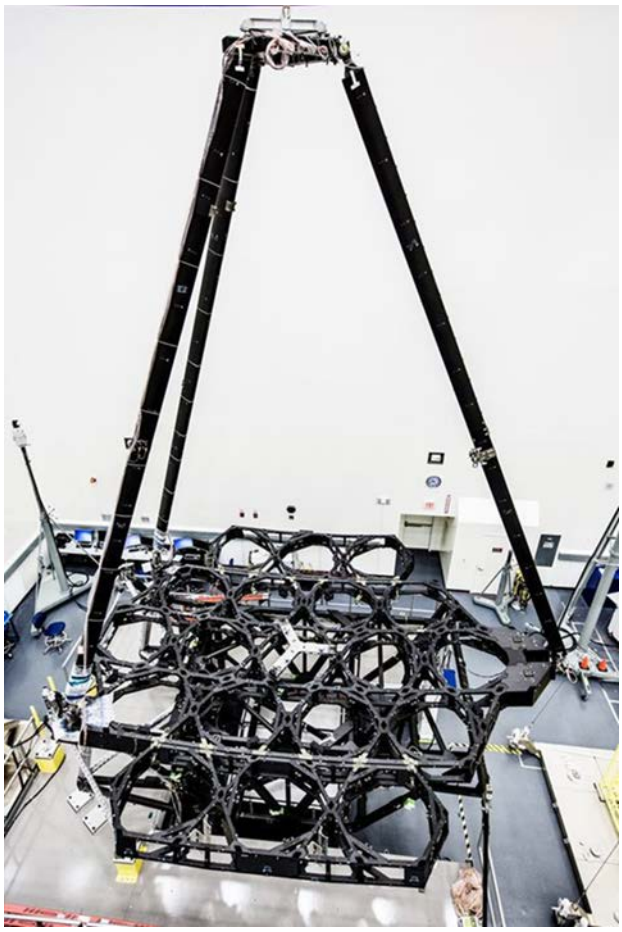

Figure 8: The telescope structure is complete and consists of more than 3200 bonded piece parts.

The telescope structure (Figure 8) consists of a M55J-954-6 cyanate ester composite material that affords a high stiffness to mass ratio and a low cryogenic expansion coefficient to yield high optical alignment stability. Approximately 3,200 bonded piece parts are assembled on a mandrel to form the structure. This structure must support launch loads and perform as a cryogenic optical metering structure. The latter function requires that it exhibit extremely low distortion upon thermal cycling over approximately 250 degrees of temperature change from ambient to its 50K operating temperature. This aspect of the structure design performance was verified through cryogenic speckle interferometry (Saif 2008).

The observatory sunshield (Figure 9) consists of five Kapton layers with shape and spacing designed to reduce the incident solar power by a factor of order 10^6. The sun facing layer is coated with silicon to prevent degradation of the substrate over the mission duration, and the remaining layers are coated with aluminum. The shield is designed with a curved dihedral shape for attitude stability and must be wrinkle free for control of stray light. As a consequence, each of 5 layers is a quilt of 50 panels that are joined with 7000 inches of seaming formed by thermal spot welds. The edge location of each panel is precisely configured to ensure that the coldest layer blocks infrared emission of warmer layers from impinging on the telescope optics. To meet this requirement, a seam-to-seam accuracy of 0.05 inches over the ~21 x 15 m assembly was achieved. Verification of the sunshield thermal design was achieved using a 1/3 scale fully functional model (Figure 9) operated in a space simulation chamber in which the L2 point solar radiation and edge view factors to cold space were simulated using lamps and cryo-panels.

4. EXTRACTING INFORMATION FROM STARLIGHT

The JWST science instrument payload contains four science instruments (Figure 10), a fine guidance sensor, and supporting systems for instrument control, command and data handling, cryogenic thermal control, and other functions (Greenhouse 2006, 2010, 2011; Lundquist 2012). Near-infrared imagery is provided by the NIRCam instrument (Rieke 2005, 2008; Beichman 2012). This camera provides high angular resolution wide-field imagery over the 0.6 – 5 μm spectrum. The detector pixel scale is chosen to optimally sample the telescope point spread function across this wavelength range by use of a dichroic beam splitter. Two identical optical modules image adjacent fields of approximately 4 square arc minutes to provide full redundancy for telescope wavefront sensing. Occulting coronography, yielding a rejection ratio of ~10^4, is provided in both long and short wavelength channels. All focal plane arrays support high cadence sub-array exposures to provide a high dynamic range capability for exoplanet transit observations.

Slit spectroscopy over the 0.6 – 5 μm spectrum is provided by the NIRSpec instrument (Bagnasco 2007; Ferruit 2012). The NIRSpec affords a range of spectral resolutions ($10^2 < \lambda/\Delta\lambda < 10^3$) that can be used with long slit, multi-object, and integral field aperture control modes. This instrument is the first aperture controlled multi-object spectrometer developed for space flight. It is designed to target 100 compact sources simultaneously within a 9 square arc minute field. Aperture control for multi-object spectroscopy is provided by an array of 250,000 micro-shutters that are configured for the desired target field based on prior NIRCam imagery. A variety of fixed long slits are provided to enable high contrast and exoplanet transit spectroscopy. Integral field spectroscopy is provided over a 9 square arc second field via an image slicer.

Near-infrared slitless spectroscopy and non-redundant mask interferometry is provided by the NIRSS instrument (Doyon 2012). This instrument provides slitless grism spectroscopy at spectral resolutions of approximately 150 and 700 over a 5 square arc minute field of view. These two grism modes are optimized for deep Ly-alpha galaxy surveys and high precision transit spectroscopy of extrasolar planets respectively. This instrument also provides sparse aperture interferometric imagery (Sivaramakrishnan 2012) via a 7 aperture non-redundant pupil mask and three broad-band filters centered on 3.8, 4.3, and 4.8 microns wavelength over which the telescope point spread function is Nyquist sampled by the NIRISS pixel scale.

Figure 9: Left -- A 1/3 scale fully functional model of the sunshield was used for design verification in a cryo-vacuum chamber equipped with solar simulator lamps; Right -- A full scale engineering model of the sunshield.

The NIRSS shares an optical bench with the FGS. The latter is a fully redundant very broad-band (0.6 – 5 um) camera that functions as the fine guidance sensor for the spacecraft attitude control and telescope fine steering mirror systems. It delivers guide star centroid measurements with a noise equivalent angle of 4 milliarcseconds (10^{-6} deg) at a rate of 16 Hz. Its wide field of view enables 95% probability of guide star acquisition over the whole sky and autonomous pattern recognition for guide star identification.

Imagery and spectroscopy over the 5-29 μm spectrum is provided by the MIRI instrument (Wright 2008). This instrument provides broad-band imagery, low spectral

resolution (1%) long slit spectroscopy, and medium spectral resolution (~10^3) integral field spectroscopy. The imaging mode includes both occulting and quadrant phase mask coronography. The latter type enables very small inner working angle observations of stellar debris disks and exoplanet systems. When used in combination with the NIRSpec instrument, an optimally sampled integral field spectrum covering the whole 0.6 – 29 μm JWST wavelength range can be obtained at medium spectral resolution.

The detectors for the JWST instruments define the state of art for high performance space flight infrared imaging arrays. The near-infrared instruments utilize HgCdTe 4 Mega pixel (Mpixel) sensor chip arrays (SCA) operated at ~40 K. Zodiacal background limited sensitivity is achieved in all broad-band instrument modes over the 0.6 – 10 μm spectrum. The MIRI instrument utilizes Si:As 1 Mpixel SCAs operated at ~6.8 K. Significant gains in noise performance and SCA format were achieved over the prior mission state of art (HST/NICMOS & Spitzer/IRAC) during the JWST technology development phase to enable the above mission science goals. The near-infrared SCAs are designed to be edge-butted on three sides to form larger format focal plane array (FPA) assemblies. The NIRCam short wavelength channel utilizes a 16 Mpixel FPA consisting of 4 of these SCAs, and the NIRSpec utilizes an 8 Mpixel FPA consisting of 2 SCAs. The mid-infrared SCAs are used individually in 1 Mpixel FPA assemblies.

5. MAKING SURE THAT IT ALL WORKS

Testing at the scale and operating temperature of the JWST requires the largest deep cryogenic (~20K) space simulation facilities in the world. The system is built up and tested in incremental steps in which each subunit is tested in a simulated flight environment before it is integrated into the next higher level of assembly (Kimble 2012, 2018). As this integration and test process proceeds, larger and larger environmental test facilities are needed. The JWST space vehicle consists of three system elements: the Optical Telescope Element (OTE), the Integrated Science

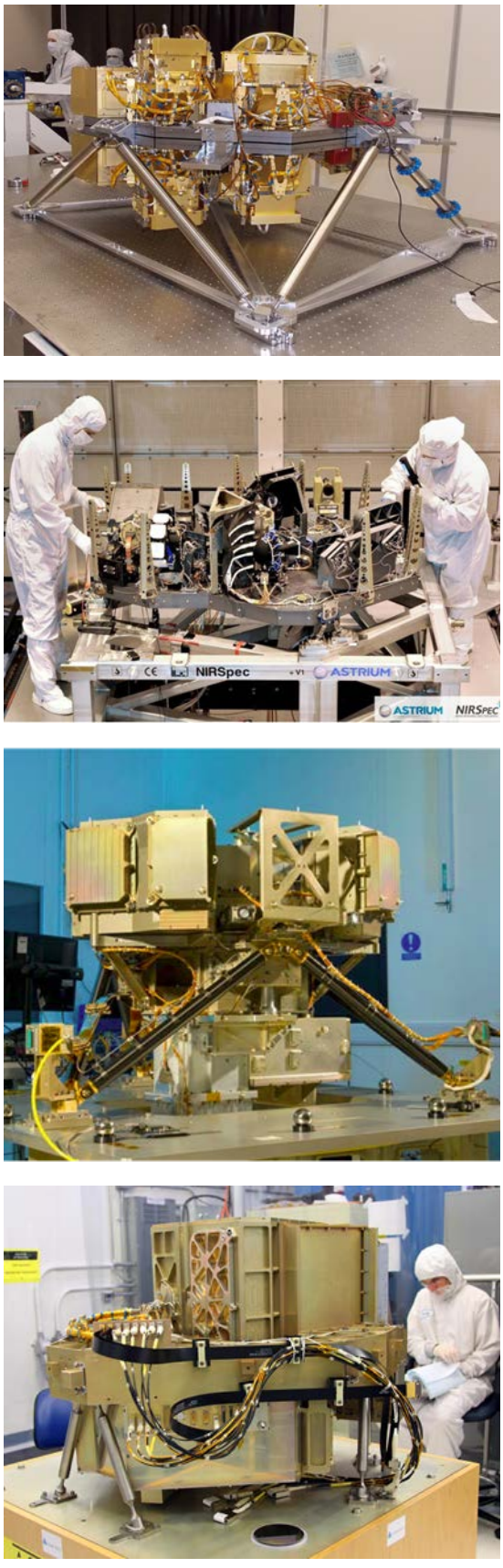

Figure 10: The JWST science instruments. From top to bottom: NIRCam, NIRSpec, MIRI, and FGS/NIRSS

Instrument Module (ISIM), and the Spacecraft Element (which includes the sunshade). When the above process of incremental testing reached the element level of assembly, the largest test facilities in the world were needed.

The first element-level test in the JWST Program was that of the ISIM. The ISIM was flight qualified at Goddard Space Flight Center using a high fidelity cryogenic telescope simulator (OSIM) (see: Hagopian 2007, Ohl 2009) and a 27 x 40 ft cryo-vacuum chamber equipped with a ~20K helium shroud to enable testing at the ISIM operating temperature (Figure 11).

The OTE structure was cryogenically tested at Marshall Space Flight Center (who also performed all cryogenic testing of the OTE primary mirror segments). The OTE was integrated at Goddard (Figure 13) using the Space System Development and Integration Facility (SSDIF) (see: Mathews 2015) – among the largest laminar flow clean rooms in the world. The OTE and ISIM elements were integrated with each other in the SSDIF and were then shipped to Johnson Space Center for end-to-end optical testing at the flight operating temperature in a 65 x 120 ft cryo-vacuum chamber (Figure 14) that has been extensively refurbished from NASA's Apollo program for JWST (Feinberg 2010, 2011; Hadaway 2018; Lightsey 2018; Irvin 2018). The OTE/ISIM was then be shipped to Northrop Grumman Aerospace Systems in Redondo Beach California for integration with the Spacecraft Element. The fully integrated JWST space vehicle will then be transported by ship to the European Space Agency's Kourou Launch Center in French Guiana for integration with the Arian 5 launch vehicle.

The above shipments will utilize the Space Telescope Transporter for Air Road and Sea (STTARS) shown in Figure 15. For shipments between GSFC, JSC, and Northrop Grumman, the STTARS will be transported by a C5 aircraft. Transport to Kourou will utilize a roll-on-roll-off transport ship. The planned route via the Panama Canal is a journey of 6,900 nautical miles that will require approximately 20 days to complete.

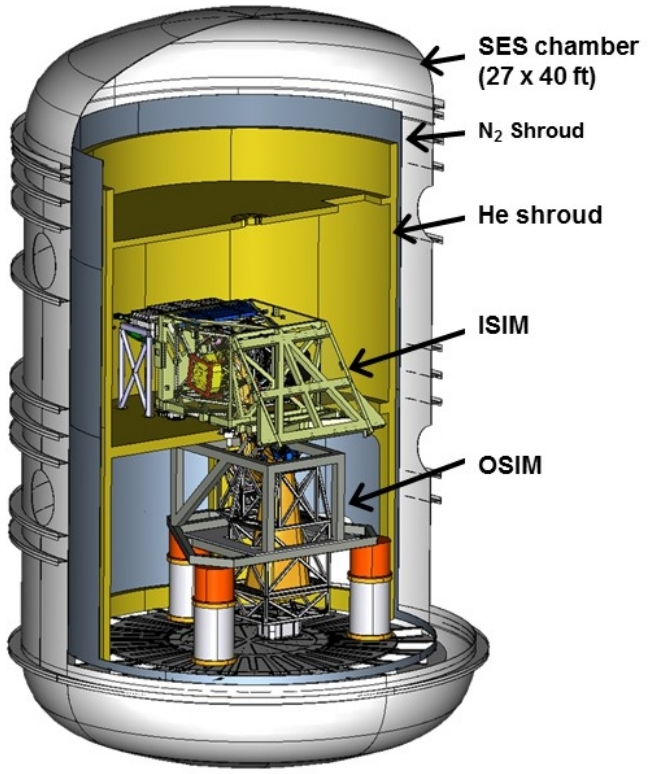

Figure 11: The cryo-vacuum test configuration for the science instrument module (ISIM) is shown in the Space Environment Simulator (SES) using the JWST telescope simulator (OSIM).

Unlike the Hubble Space telescope, which resides in low earth orbit, the JWST cannot be serviced by astronauts due to its more distant Sun-Earth L2 point orbit. However, in contrast to prior space observatories, the JWST telescope and instrument optical systems employ a high degree of capability for in-flight adjustment (Barto 2008), and lessons learned from prior observatory test programs are carefully taken into account in design of the above test program (Feinberg 2008).

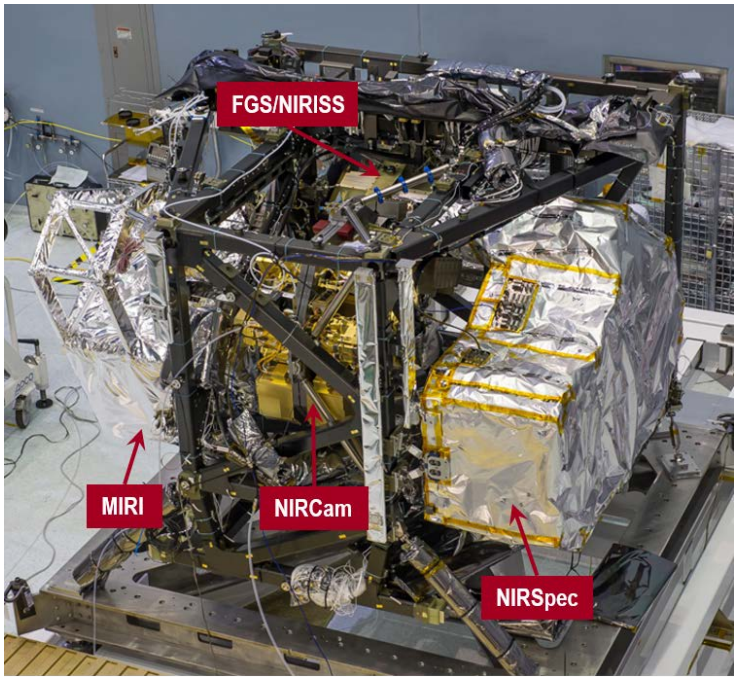

Figure 12: The science instrument module is shown at 100% integration.

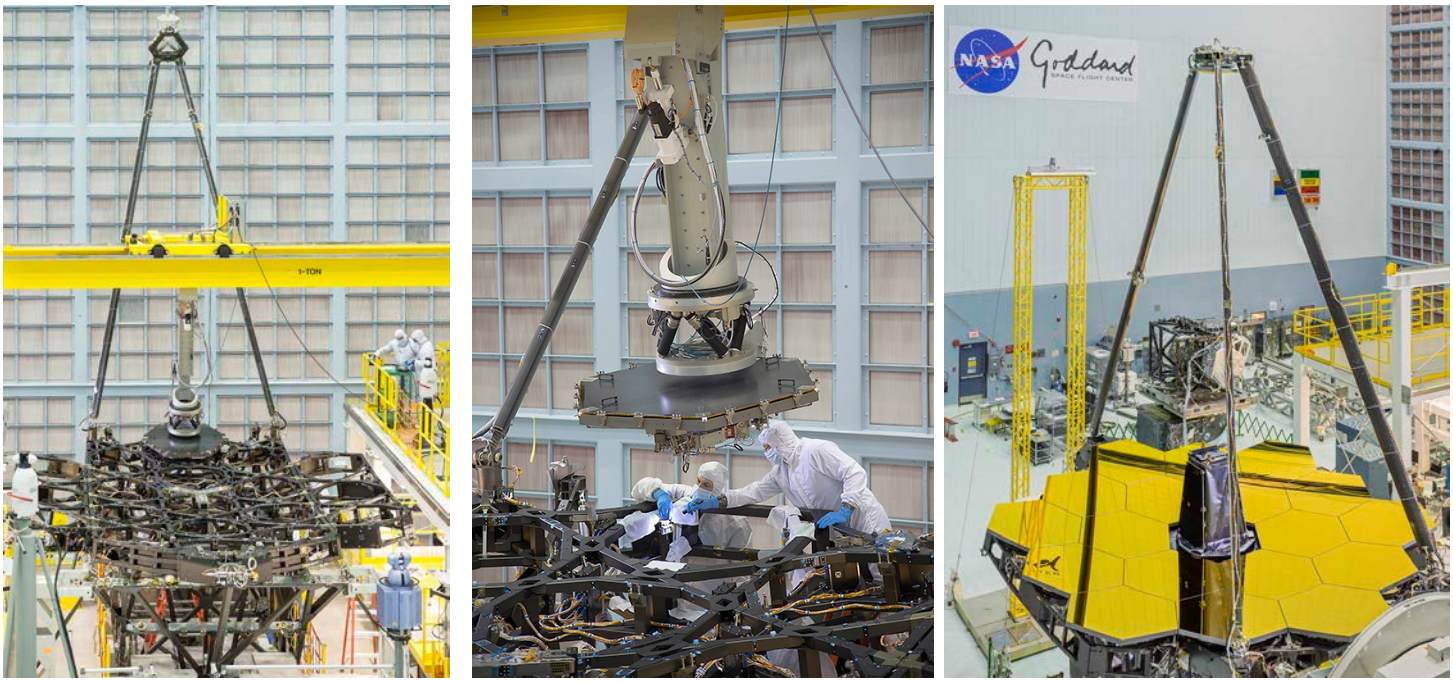

Figure 13: Left and center: Integration of the first flight primary mirror segment to the telescope structure is shown using the Ambient Optical Assembly Stand in the GSFC Space System Development and Integration Facility. Right: the fully integrated primary mirror. See Mathews, et al, 2015 for further details.

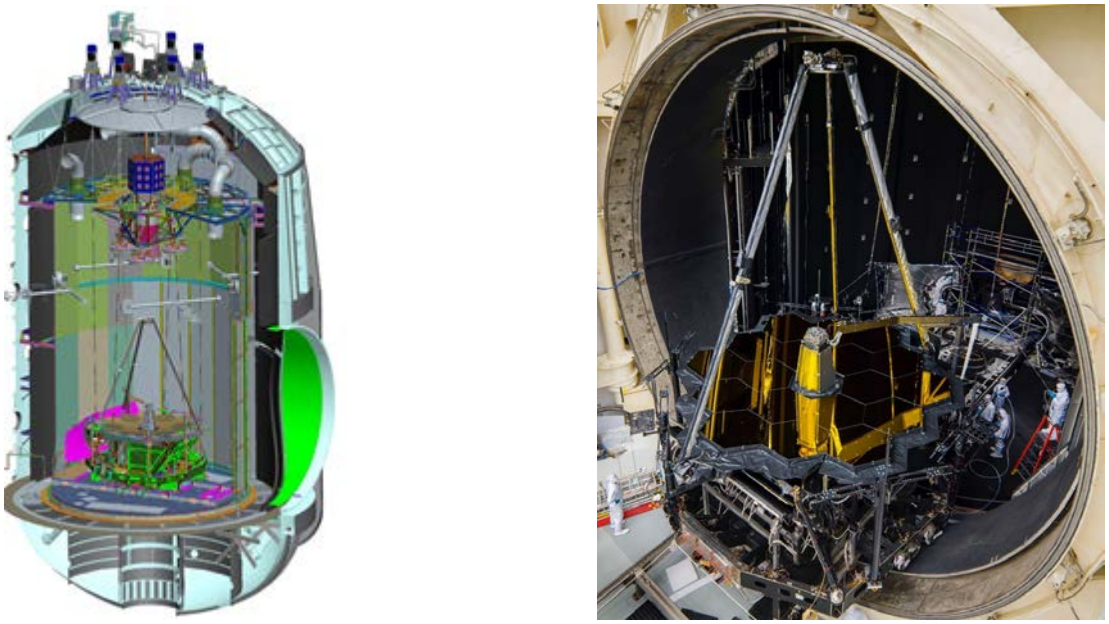

Figure 14: Left -- The JWST end-to-end optical test configuration in Johnson Space Flight Center Chamber A; Right – the flight observatory entering the test chamber.

Figure 15: Top -- The Space Telescope Transporter for Air Road and Sea (STTARS); Lower left -- STTARS being loaded into a C5 aircraft; Lower right -- The ship that will carry STTARS from Los Angeles to French Guiana.

6. REFERENCES

Acton, D.S., et al., 2012, "Wavefront Sensing Controls for the James Webb Space Telescope," Proc. SPIE, 8442-87.

Acton, D.S., et al., 2004, "James Webb Space Telescope Wavefront Sensing and Control Algorithms," Proc. SPIE, 5487, 877.

M. Albanese, A., et al., 2006, "Verification of the James Webb Space Telescope coarse phase sensor using the Keck Telescope," Proc. SPIE 6265.

Beichman, C. A., et al., 2012, "The Near-Infrared Camera for the James Webb Space Telescope: Status and Science Goals," Proc. SPIE, 8442-93.

Bagnasco, G. et al. 2007, "Overview of the near-infrared spectrograph instrument on-board the James Webb Space Telescope," Proc. SPIE, 6692, 17.

Barto, A., et al., 2008, "Optical performance verification of the James Webb Space Telescope," Proc. SPIE, 7010, 23.

Contos, A., et al., 2008, "Verification of the James Webb Space Telescope (JWST) wavefront sensing and control system," Proc. SPIE, 7010, 26.

Doyon, R., et al., 2012, "The JWST Fine Guidance Sensor (FGS) and Near-Infrared Imager and Slitless Spectrograph (NIRISS)", Proc. SPIE, 8442.

Feinberg, L., et al., 2012, "James Webb Space Telescope optical telescope element mirror development history and results," Proc. SPIE, 8442, 82.

Feinberg, L., et al., 2011, "James Webb Space Telescope system cryogenic optical test plans," in Cryogenic Optical Systems and Instruments XIII, Aug 24-25, San Diego, CA 2011, 815007.

Feinberg, L., et al., 2010, "Use of a pathfinder optical telescope element for James Webb Space Telescope risk mitigation", Proc. SPIE 7731, 77313T.

Feinberg, L., et al., 2008 "Applying HST lessons learned to JWST," Proc. SPIE, 7010, 13.

Feinberg, L., et al., 2007, "TRL-6 for the JWST wavefront sensing and control," Proc. SPIE, 6687.

Ferruit, P., et al., 2012, "The JWST Near-Infrared Spectrograph NIRSpec: Status," Proc. SPIE, 8442, 94.

Gallagher, B., et al., 2011, "JWST Mirror Production Status", Proc. SPIE 8146, 814607.

Gardner, J. P., 2012, "Science With the James Webb Space Telescope", Proc. SPIE 8442, 79.

Gardner, J. P., et al., 2006, Space Sci. Rev., 123, 485

Greenhouse, M.A., et al., 2011," Status of the James Webb Space Telescope integrated science instrument module system," Proc. SPIE 8146, 262.

Greenhouse, M.A., et al., 2010," Status of the James Webb Space Telescope integrated science instrument module system," Proc. SPIE 7731, 108.

Greenhouse, M. A., et al., 2006, "The James Webb Space Telescope Integrated Science Instrument Module," Proc. SPIE 6265, 33.

Hadaway, James B., et al., "Performance of the center-of-curvature optical assembly during cryogenic testing of the James Webb Space Telescope," Proc SPIE, Vol. 10698.

Hagopian, J., et al., 2007 "Optical alignment and test of the James Webb Space Telescope Integrated Science Instrument Module," IEEE Aerospace Conference, 3—10 Mar 2007, Big Sky, Montana.

Jason Kalirai (2018) Scientific discovery with the James Webb Space Telescope, Contemporary Physics, 59:3, 251-290.

Kimble, R. A., et al., 2012 "The Integration and Test Program of the James Webb Space Telescope," Proc. SPIE 8442-90.

Kimble, R. A., et al., 2018 James Webb Space Telescope (JWST) optical telescope element and integrated science instrument module (OTIS) cryogenic test program and results, "Proc. SPIE, Vol 10698.

Lightsey, P., et al, 2018 "James Webb Space Telescope optical performance predictions post cryogenic vacuum tests," Proc. SPIE, Vol. 10698.

Lightsey, P., et al., 2012 "James Webb Space Telescope: large deployable telescope in space", Opt. Eng., 51, 011003.

Lundquist, R., et al., 2012, "Status of the James Webb Space Telescope integrated science instrument module system," Proc. SPIE 8442, 92.

Matthews, G. W., et al., 2015 "JWST Pathfinder Telescope Integration," Proc. SPIE 9575, 957504-1.

Ohl, R., et al., "Updates to the optical alignment and test plan for the James Webb Space Telescope Integrated Science Instrument Module," Proc. SPIE, in press.

Rees, M. J. 1997, in N. R. Tanvir, A. Aragon-Salamanca, & J. V. Wall eds., The Hubble Space Telescope and the High Redshift Universe, (World Scientific: Singapore), 115

Rieke, M., 2005," Overview of James Webb Space Telescope and NIRCam's Role," Proc. SPIE, 5904, 1.

Rieke, M., 2008, see: http://ircamera.as.arizona.edu/nircam/AAS_June08.pdf

Rigby, J., et al., "Science Operations With the James Webb Space Telescope," Proc. SPIE, 8442, 80.

Saif, B., et al., 2008, "Measurment of Large Cryogenic Structures Using a Spatially Phase-Shifted Digital Speckle Pattern Interferometer," Applied Optics, 47, 737.

Sivaramakrishnan, A., "Exoplanet and Black Hole Science with Non-Redundant Interferometric Masks on JWST," Proc. SPIE, 8442, 98.

Wright, G., et al., 2012, "Overview of MIRI Status and First Indications of Flight Performance," Proc. SPIE, 8442, 95.

Wright, G., et al., 2008, "Design and development of MIRI, the mid-IR instrument for JWST," Proc. SPIE, 7010, 27

7. BIOGRAPHY

Matt Greenhouse received a BS in geosciences during 1979 and a PhD in astrophysics during 1989. After receiving his doctorate, he joined the Smithsonian Institution in Washington, DC as a staff astrophysicist and joined Goddard Space Flight Center during 1996 in the same capacity. He has served as project scientist for the JWST science instrument payload since 1997.